Can an Atomic Force Microscope Sequence DNA Using a Nanopore?

Shahid Qamar,* Phil M. Williams,† and S. M. Lindsay*
*Center for Single Molecule Biophysics, The Biodesign Institute, Arizona State University, Tempe, Arizona 85287; and †Laboratory of Biophysics and Surface Analysis School of Pharmacy, University of Nottingham, Nottingham, NG7 2RD, United Kingdom

ABSTRACT R. Bension has proposed that single molecules of DNA could be sequenced rapidly, in long sequential reads, by reading off the force required to pull a tightly fitting molecular ring over each base in turn using an atomic force microscope (AFM). We present molecular dynamics simulations that indicate that pulling DNA very rapidly (m/s) could generate large force peaks as each base is passed (~1 nN) with significant differences (~0.5 nN) between purine and pyrimidine. These speeds are six orders of magnitude faster than could be read out by a conventional AFM, and extending the calculations to accessible speeds using Kramers' theory shows that thermal fluctuations dominate the process with the result that purine and pyrimidine cannot be distinguished with the pulling speeds attained by current AFM technology.

INTRODUCTION

Knowledge of the complete sequence of a human genome can help in early detection of genetic diseases, improved diagnosis of disease, and rational drug design (1–5). Obtaining the full sequence is, however, a difficult task. The present method of sequencing, based on Sanger's method (6), is reliable but slow and expensive and cannot readily map out repeated sequences. The advent of nanotechnology in the biological sciences has led to proposals for several new methods for fast and inexpensive DNA sequencing. Among the proposals, DNA sequencing through a nanopore has received significant attention in the scientific community. DNA translocation through a nanopore in a membrane was first studied by Kasianowicz et al. in 1996 (7). The diameter of single-stranded DNA is ~1–2 nm, so it cannot pass through a nanopore of size ~0.6 nm easily.

The basic idea behind nanopore sequencing is the use of simultaneous measurement of ion current through the pore (or measurement of the speed of translocation) as a function of sequence when a single strand of DNA passes through a pore. A voltage applied across a nanopore causes a charged, single-stranded DNA molecule to transit through the nanopore. Pores can be fabricated in solid-state devices (8), in nuclear membranes (9), or using molecular rings, for example cyclodextrin (CD) (10,11). Previous studies have focused on measuring the change in ionic current as a single strand of DNA transited through a pore (8,9). However, the base-dependent signal was found to be too weak for practical purposes. Additionally, a collective motion of bases was observed that precluded single-base readout.

Bension (12) has proposed a technique to sequence DNA based on the mechanical translocation of a CD rotaxane along ssDNA (10). CD is a cyclic oligosaccharide composed of six (α-CD), seven (β-CD), or eight (γ-CD) 1-4-linked α-D-glucopyranoside units. Simple modeling suggests that a nucleotide containing a pyrimidine should pass through a β-CD, whereas a nucleotide containing a purine would be obstructed. In the method proposed by Bension (12), a single-stranded DNA molecule is threaded through a β-CD ring. The ring is pulled over the DNA using an AFM tip covalently bound to the CD. Such a structure has been built and tested (Q. Spadola, S. Qamar, P. Zhang, G. Kada, R. Bension, and S. M. Lindsay, unpublished data). Here, we focus on computational and theoretical modeling of the experiment. We begin with simple steered molecular dynamics (SMD) simulations. These are incapable of reaching out to the approximately millisecond timescales of AFM readout, so we then turn to a fuller calculation based on Kramers' theory. The simulations must include the calculation of the free energies for the DNA CD rotaxane using a milestoning method (13) and rate kinetics of the system using master kinetic equations (14). The diffusive motions of the rotaxane were studied previously (15) to calculate the friction and diffusion coefficients of the molecule. In this study, we present the experimental strategy as shown in Fig. 1, molecular modeling, computation of free energies and kinetics rates, and finally predict the forces required by the CD ring to cross over the bases.

SMD SIMULATIONS

SMD simulations were performed for our model system to estimate the friction and diffusion coefficients. All simulations were performed in explicit water. Four models were made; one for each base A, G, T, and C complexed as a rotaxane with β-CD as shown in Fig. 2. All simulations were done using the classical force field AMBER 94 (16). Additionally, some were repeated in the CHARMM 27 force field (17). The NAMD (18) program was used for all simulations. The initial structure was made by creating a model for each base A, G, T, and C rotaxane complex separately in AMBER 6.0 (19). The initial structure for the

Submitted March 13, 2007, and accepted for publication September 14, 2007.

Address reprint requests to Shahid Qamar, Center for Single Molecule Biophysics, The Biodesign Institute, Arizona State University, Tempe, AZ 85287. E-mail: shahid.qamar@asu.edu.

Editor: Jose Onuchic.

0006-3495/08/02/1233/08 $2.00

doi: 10.1529/biophysj.107.108670

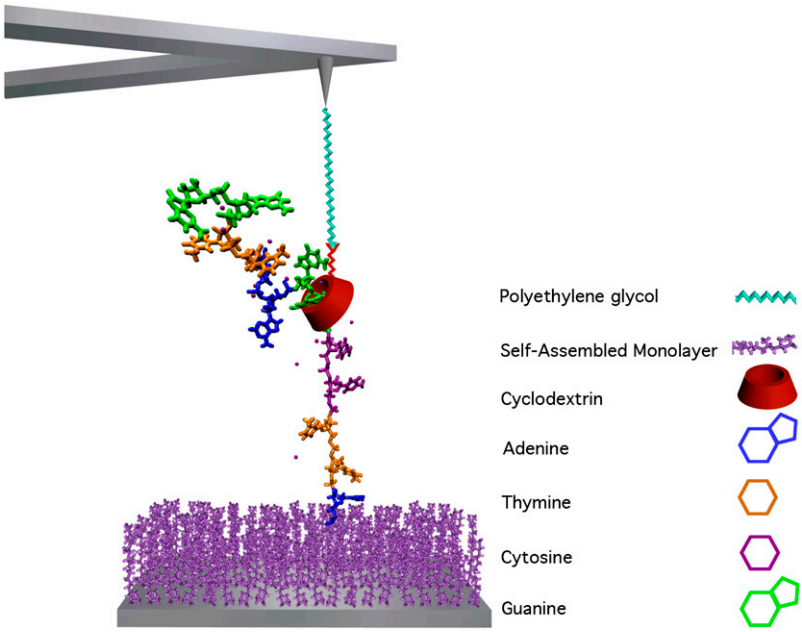

FIGURE 1 Schematic of the DNA rotaxane assembly for the nanopore DNA sequencing. The color scheme explains each component. A CD (*red*) is being pulled along the ssDNA strand with a functionalized AFM tip. In the experimental setup, a second long PEG molecule is used as a spacer between the surface and the DNA (not shown here).

CD ring was taken from RCSB protein data bank and was parameterized in AMBER 7.0. To calculate the frictional forces, all the models consisted of a CD initially threaded by a poly(polyethelyne glycol) (PEG) molecule that has DNA bound to one end, as shown in Fig. 2. Na^+ ions were added to balance the negative charges on the phosphates. Each system was solvated in the TIP3P water model (20), minimized, and equilibrated in the NPT ensemble using Nose Hoover Langevin piston pressure control (21). A constant temperature of 300 K and a pressure of 1 bar were maintained with the Berendsen thermostat (22) and Langevin piston barostat (23), respectively. The velocity-Verlet algorithm (24) with a single time step of 2 fs was used in the time integration. Hydrogen bonds were constrained with a SHAKE algorithm (25).

In the experiment, an AFM tip, functionalized with a PEG tether and vinyl sulfone reactive group, is brought near the surface to bind with a functionalized CD. When the tip is retracted from the surface, it pulls the CD with it. If the CD experiences different forces as it is pulled over either purine or pyrimidine, the purine-pyrimidine sequence could be read out. In the SMD, this pulling is simulated by applying a force to one of the oxygen atoms in the CD. A theoretically simulated force curve (for passing an adenine base at rate of 1 m/s) is shown in Fig. 3.

THEORY FOR THE KRAMERS' SIMULATIONS

As will become evident, SMD is inadequate for the problem at hand. We used the Evans' theory of dynamic force spectroscopy (26) to find the forces required for the CD to cross over a purine or pyrimidine at rates more appropriate to the AFM experiment. From this theory (27), the most probable force will be

$$f^* = k_B T / x_u \ln(r_f X_u / k_B T \upsilon o), \quad (1)$$

where υ_o, the rate of barrier crossing, is given by $k_o \exp(\Delta E / k_B T)$. k_o is the prefactor of Kramers' theory, ΔE is the free energy barrier at the transition state, and k_B is the Boltzmann constant. x_u is the distance to the transition state. The force f^* needed to pull the CD over the base depends on the loading rate r_f, distance to the transition state x_u, the activation energy barrier ΔE, and the diffusive rate constant υ_o.

For the purpose of estimating rates, we will take the distance to the transition state to be ~0.2 nm (a full energy landscape is presented later in this article). To use Eq. 1, we need to calculate the activation energy barrier, ΔE, and the diffusion rate, $k_0 = 1/t_D$. These quantities were calculated using the milestoning technique developed by Elber and Faradjian (13) as described here.

PARAMETERS AND MEASUREMENTS

DNA threading CD at constant speed

We simulated the single-stranded DNA molecule with a CD ring as a threading pore. We modeled a single nucleotide attached to one end of a PEG molecule (MW 262) aligned such that the PEG passes through the center of the CD (as shown in Fig. 2).

One end of the PEG molecule was constrained so that it did not move during the SMD simulations. The CD ring was pulled at different constant speeds, and force curves were obtained from the simulated data. We collected the pull-off forces (i.e., the peak force in curves like that shown in Fig. 3) for all four nucleotides. The peak forces at each speed are listed in Table 1 and plotted in Fig. 4. Note that the plots of peak force versus pulling speed are linear (i.e., obey Stokes's law), implying that the SMD simulations are dominated by molecular friction and not by thermally activated hopping. This is a clear indication that the results of these simulations are not appropriate for the (much slower) AFM experiments.

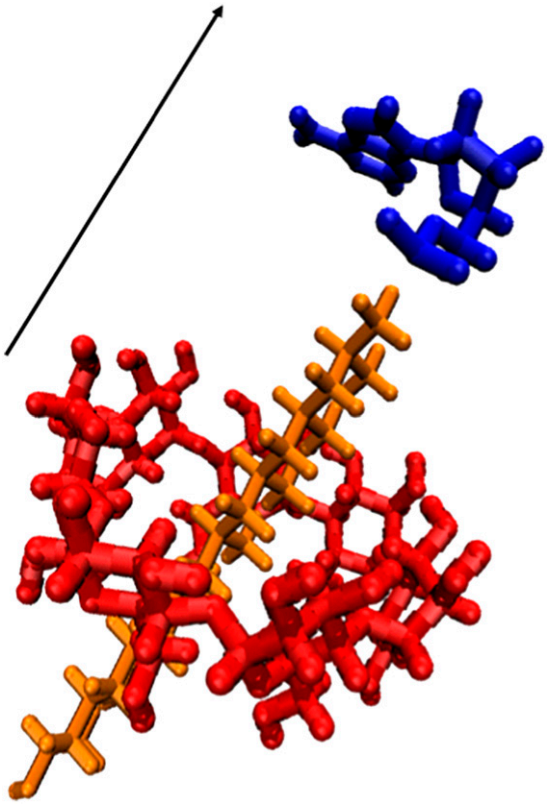

FIGURE 2 DNA rotaxane model for constant-speed SMD simulations. The PEG molecule (*orange*) is attached to a single base adenine (*blue*). The second end of the PEG molecule is fixed. The arrow shows the pulling direction for the CD (*red*).

Nonetheless, these data are useful because the molecular friction coefficients may be estimated from the slopes of the plots in Fig. 4. The friction coefficients, ζ, are 684 (purine) and 260 (pyrimidine) pN-s/m. In principle, these friction coefficients can be used to estimate the barrier-crossing kinetics, and we compare the milestoning approach with estimates obtained from these friction coefficients below.

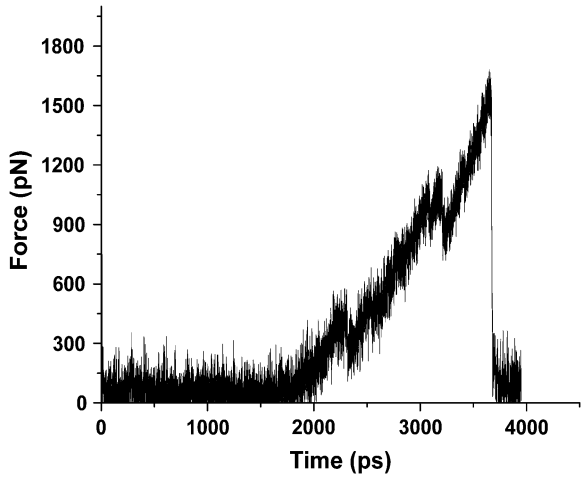

FIGURE 3 Typical force curve profile from SMD obtained at a speed of 1 m/s when a single adenine nucleotide of ssDNA was threaded through a CD ring. The three force peaks show when the CD leaves PEG, sugar, and the base, respectively.

TABLE 1 Peak forces for the CD to pass each of the bases as a function of pulling speed at constant pulling speed

Speed (m/s)	A (pN)	G (pN)	C (pN)	T (pN)
0.2	230	300	100	120
0.3	300	350	120	150
0.4	350	400	150	180
0.5	425	500	210	260
0.6	500	580	315	380
1	700	600	400	450

Threading at constant force

We took the same model and threaded the DNA molecule at constant force. We applied three different forces to the CD ring and waited until it passed over a base. We calculated the time it took for the CD to slip over the base, and, using the 0.6-nm separation of bases in stretched DNA (28), we computed the speed at which the CD passed over the base. The data obtained from constant force using the AMBER force field for the same model are shown in Table 2. Comparison of Table 1 (constant speed) and Table 2 (constant force) shows that we get similar translocation speeds using the two different methods. The forces required to pull the CD over a base are large at these pulling speeds, and the difference between the forces predicted for purine and pyrimidine is significant in this molecular-friction-dominated regime.

Calculations of activation energy and rate kinetics

As discussed in the introductory section, SMD pulling speeds are six orders of magnitude faster than the conventional AFM speeds. To bridge the molecular dynamics simulations

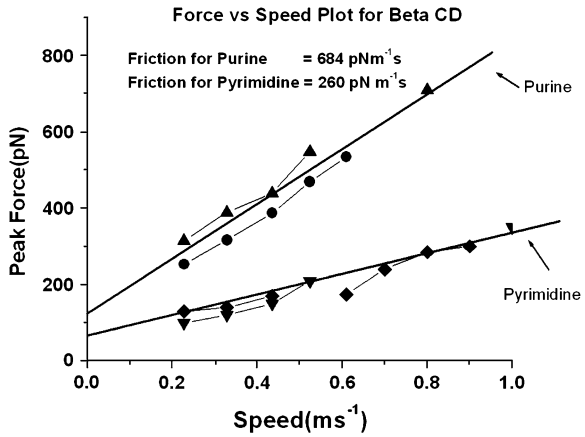

FIGURE 4 Force-versus-speed plot calculated with SMD for β-CD passing over a purine (*triangles*, *G*; *dots*, *A*) and a pyrimidine (*triangles*, *C*; *diamonds*, *T*). The slopes yield the friction coefficients as 684 pN ms^{-1} for purine and 260 pN ms^{-1} for pyrimidine.

TABLE 2 Effective speed at which a CD rotaxane passes an adenine nucleotide as a function of (constant) applied force

Speed (m/s)	Force (pN)
0.2	300
2	680
7	1056

with AFM experiments, i.e., to get the AFM speeds or AFM forces from molecular dynamic simulations, we used Kramers' theory, which gives AFM forces at realistic speeds using the activation energy barriers and rate kinetics as inputs. Here we adopted the technique known as milestoning developed by Elber and Faradjian (13) to calculate the activation energy for passage of a CD rotaxane and the kinetic rates of the system. This procedure involves running molecular dynamics simulations at the microsecond level to catch rare events in biological motion. We divided the whole space between initial and final states into equally spaced milestones, which are the hyperplanes perpendicular to the reaction coordinates. These milestones are situated at 0.5 Å from each other, the distance that a CD has to travel in a random walk before it makes it to the next or previous milestone. A schematic of the milestones is shown in the Fig. 5. The choice of milestone separation was checked by running the calculations at a number of different milestone separations to ensure that local equilibrium was obtained with the milestones used.

CHOICE OF REACTION COORDINATES

Choice of the appropriate reaction coordinate is critical in milestoning. Motion along the chosen reaction coordinate must be slower than all other degrees of freedom so that the system reaches its statistical equilibrium more slowly than for other degrees of freedom. In this one-dimensional system, the obvious choice of reaction coordinate is the direct path for which the CD is centered on the DNA backbone, and indeed, we found that motions along this path were slower than motions in the perpendicular direction. After minimization and equilibration, we ran Brownian dynamics simulations on the CD placed between two adenine bases and observed the motion of the center of mass of the CD along and perpendicular to the backbone of the ssDNA molecule.

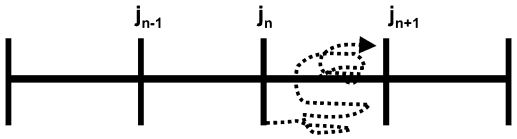

FIGURE 5 Schematic of the milestones separated by 0.5 Å. A trajectory initiated at j_n milestones terminates at j_{n+1} milestone shown in a dotted line. The vertical lines are hypersurfaces perpendicular to the reaction coordinates.

An interval of 300 ps of the simulation is shown in Fig. 6, where the red trajectory is for motions perpendicular to the backbone and the blue trajectory is for motions along the backbone.

We used the Arrhenius rate equation to calculate the local activation energy at each milestone:

$$\Delta E = -k_B T \ln(k_f/k_r). \quad (2)$$

Here k_f and k_r are the forward and reverse rates at a particular milestone. Instead of running one big simulation, we ran small trajectories at each milestone, i.e., j_n and calculated the times it takes for a trajectory to make it to adjacent milestones, i.e., $j + 1$ or $j - 1$.

A total of 500 trajectories were run at each milestone. To compute the first passage time distribution, histograms of trajectories were repeatedly reconstructed using successively smaller bin widths in time until they converged, i.e., when further reduction in the bin size and an increase in the number of trajectories did not change the simulation results, as shown in Fig. 7.

To calculate the kinetics of the system, we used the master equation

$$dP_i(t)/dt = \sum_{j=0}[P_j(t)k_{ji} - P(t)k_{ij}], \quad (3)$$

where $P_i(t)$ is the probability of the system being in state i at time t, and k_{ij} is the transition probability from state i to state j. $P_i(t)$ can also be described as the population of the states at each milestone, and k as the forward and reverse rate constants. A Markov process (29–31) is used to describe the Brownian motion of the CD. Following the Markov process, the CD makes a transition from the milestone j to $j + 1$ and $j - 1$ with rate constant of k_f and k_r for the forward and reverse transitions, respectively. The nonzero transition probability satisfies the detailed balance condition

$$k_{ij}/k_{ji} = \exp(-\Delta E_{ij}/k_B T). \quad (4)$$

We calculated the forward and reverse rate constants after running 500 small trajectories at each milestone for a total of 7500 trajectories for the 15 milestones shown schematically in Fig. 8. The CD was started from an equilibrium position in the middle of a row of four adenine nucleotides and followed until it passed to a new equilibrium position between the third and fourth adenines on the oligomer.

To calculate the kinetics of the system, we have to solve the master equation numerically. We considered the rate constant for flow of probability across a division of configuration space into two equal and symmetric halves (containing states A and B). Here state A is the equilibrium state on the left of the transition state and state B is at milestone 11, just to the right of the transition state. The rate of reaction k_0 (the Kramers' rate constant) from A and B was computed assuming two-state kinetics

$$k_0 t = -\ln(1 - P_B). \quad (5)$$

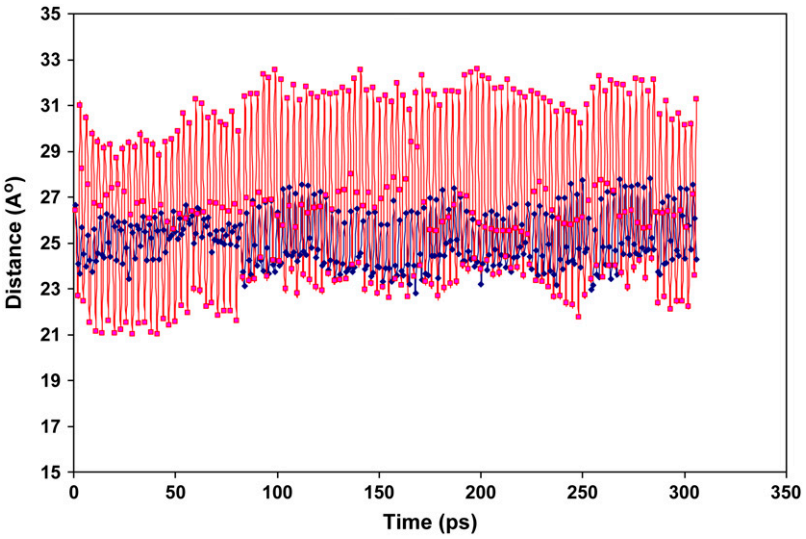

FIGURE 6 Simulated Brownian motion of the center of mass of the CD in directions along (*blue*) and perpendicular (*red*) to the backbone of DNA with the CD at its equilibrium position between two adenine bases.

In the above equation, P_B is the normalized probability of state B.

RESULTS

Energy profile from milestoning data

The Arrhenius relation (Eq. 2) is used to estimate the free-energy difference between any pair of milestones, say n and $n + 1$, by inserting the ratio of $k_f(n)$ to $k_r(n + 1)$ in the exponent. The calculations started (at zero energy) with the CD equilibrated between the middle two adenines of a four-adenine oligomer and ended with the CD between the third and fourth adenines, moving along the oligomer in a 5′-to-3′ direction (see the *insets* in Fig. 9).

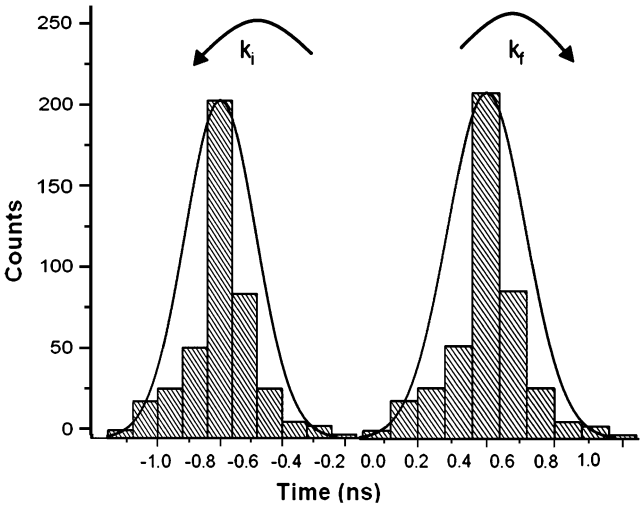

FIGURE 7 Histogram of forward and backward times of trajectories generated at a particular milestone. The k_f and k_r are the forward and reverse first passage time distributions.

The calculated energy profiles along the reaction coordinate for purine and pyrimidine are shown in Fig. 9. The free energy minima in Fig. 9 correspond to equilibrium positions of the CD ring on either side of a base. The maximum energy barrier, corresponding to the transition state, is found between milestones 10 and 11. The free energy landscape has some interesting features. It is not symmetrical, a consequence of the requirement that the base flip over to allow passage of the CD. Interestingly, the CD returns to the zero of energy after passing the smaller pyrimidine but has a somewhat higher energy after passing the larger purine, presumably because there is some residual interaction (the purine plus CD dimensions exceeding the base-to-base distance in stretched DNA).

The value of the peak free energy barrier for purine is almost twice the value found for the pyrimidine. This behavior was expected because the pore size is the same for both purine and pyrimidine, but the purine is bigger than the

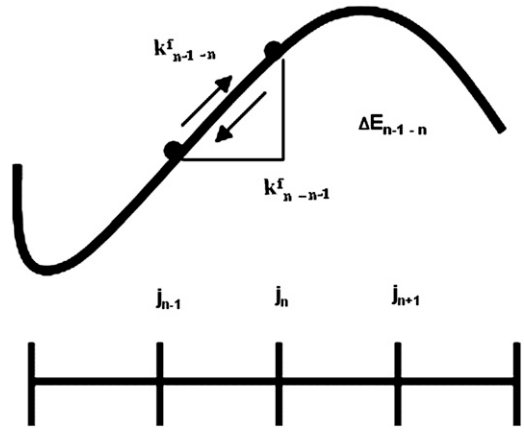

FIGURE 8 Schematic of the activation energies at each milestone. The k_f and k_r are the forward and backward rates at each milestone, and E_{n-1-n} is the energy difference between the j_{n-1} and j_n milestones.

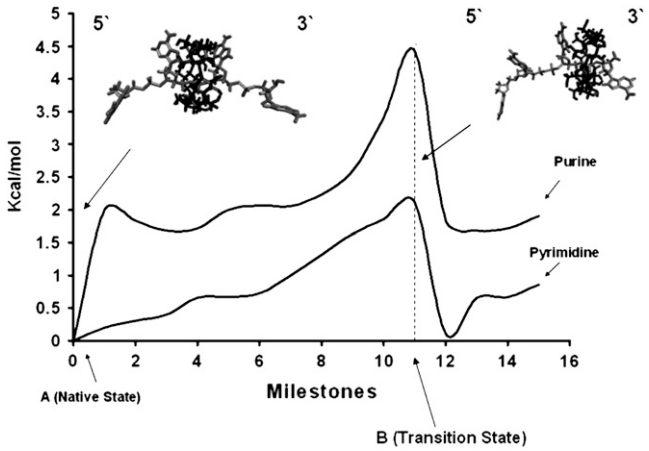

FIGURE 9 Energy profile for the passage of the CD over a purine and a pyrimidine obtained from milestoning data. The high point is the transition state. The insets show the initial and final positions of the CD, and the planes labeled *A* and *B* were used for computing transition rates over the barrier.

pyrimidine. This is consistent with the base dependence of the forces, which we calculated using SMD (Table 1).

Kientics rates from milestoning data

The numerical solution of the master equation gives us the evolution of the system over time using initial values and forward and reverse rates at each milestone. Fig. 10 shows the quantity $-\ln(1 - P_B)$ plotted as a function of time (in ns). The plots are linear and fitted with $k_0 = 1.296 \times 10^{-3}$ $(\text{ns})^{-1}$ (purine) and 1.7×10^{-2} $(\text{ns})^{-1}$ (pyrimidine). The corresponding transit times are 772 ns (purine) and 59 ns (pyrimidine).

The friction coefficients calculated from SMD can, in principle, be used to estimate transit times (15). The Einstein-Smoluchowski relation, $D = K_B T/\zeta$, yields $D = 0.6 \times 10^{-7}$ cm^2s^{-1} for the passage of a purine and 1.5×10^{-7} cm^2s^{-1} for the passage of pyrimidine. Using $t_o = l_{ts}l_n/D$ (l_{ts} and l_n are the widths under the saddle point at $K_B T$ below the transition state and the width of the well at $K_B T$ above the native state equilibrium) (32), we estimate t_o to be ~4.8 ns for the purine and 1.8 ns for the pyrimidine (for simplicity we have taken $l_{ts} = l_n$.= 0.17 nm). Using these rates as prefactors in the Arrhenius equation $\tau = t_0 \exp(\Delta E/K_B T)$ yields the transit times for purine as ~8500 ns (using $\Delta E = 4.5$ kcal/mol; Fig. 9) and for pyrimidine as 50 ns (using $\Delta E = 2$ kcal/mol; Fig. 9). The agreement for the purine is probably fortuitously good. The estimate for the pyrimidine is about a factor 11 too large. This order-of-magnitude agreement is quite encouraging for factors that are exponentially sensitive to the details of the calculations, and it suggests that our results are probably robust to within an order of magnitude. Given the final result of this article, this is adequate for our purposes.

FORCES from simulation data

From the transit times at zero force, Eq. 1 predicts the pulling rates needed for a sequence-dependent signal to be evident. For the purposes of this discussion, we will assume that the milestoning predictions of transit times of 772 ns (purine) and 59 ns (pyrimidine) are the correct values. The peak force predicted by Eq. 1 falls to zero when $r_f x_u/k_B T \upsilon_0 = 1$. This is the point where the power deposited by the AFM probe exactly equals the power dissipated by thermally driven fluctuations over the barrier. For purine, this yields $r_f\,(f = 0) \approx 2.7 \times 10^{-5}$ N/s, whereas for pyrimidine, $r_f\,(f = 0) \approx 3.6 \times 10^{-4}$ N/s. These loading rates are two orders of magnitude larger than the largest experimental loading rates (of $\sim 10^{-7}$ N/s). Using the experimental cantilever stiffness (0.3 N/m), we do not predict a significant force signal unless the pulling rate is of the order of one base per 100 ns with a barrier height of 20 $K_B T$. We also explored different loading rates, plotting the predicted peak forces in Fig. 11. It is evident from the plot that even at an extremely high loading rate

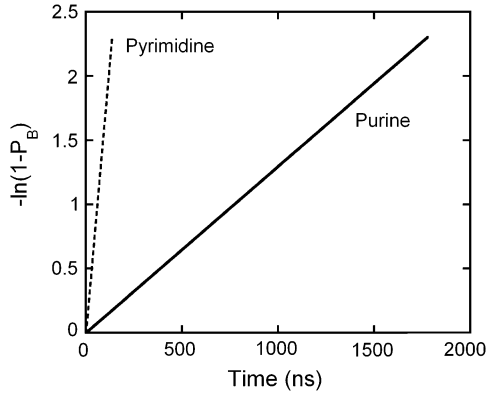

FIGURE 10 Logarithm of the normalized probability flux versus time fitted to Eq. 5 to yield the barrier-crossing rates for purine (*solid line*) and pyrimidine (*dotted line*).

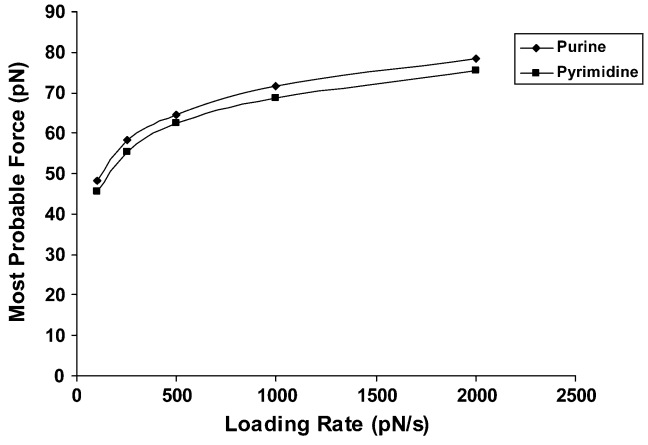

FIGURE 11 Most probable force-versus-loading rate for the CD to pass a purine and pyrimidine calculated using Eq. 1.

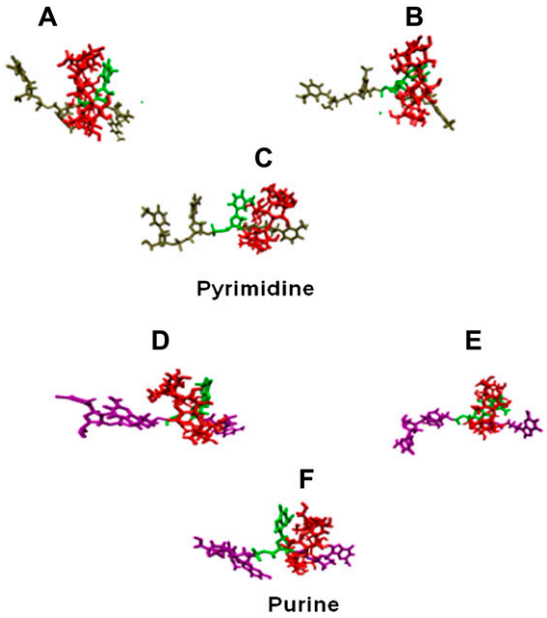

FIGURE 12 (*A–C*) Positions of the CD ring at milestones 9, 10, and 11 for passage of a pyrimidine. In the transition state (*B*) the base (*green*) is flipped over to pass through the CD (*red*). On each side of the transition state (*A* and *C*) the base is in its normal position with respect to the phophodiester backbone. (*D–F*) Smilar results for a pyrimidine (*E* is the transition state).

(2500 pN/s) the forces are between 75 pN and 78 pN, close to the AFM noise level of 50 pN (as observed in experiments at much slower pulling rates). Although it may be possible to pull and read at much higher loading rates, the experiments were limited by the need to pull slowly enough for the CD to pass the PEG tether that held the DNA to the substrate, so this option is not currently available.

DISCUSSION AND CONCLUSIONS

The activation energies for passing a purine or a pyrimidine calculated in this study are of the order of a few times k_BT. In consequence, fluctuations dominate the passage of the bases through the CD at timescales relevant to AFM experiments, and large differences in the molecular friction between purine and pyrimidine are found only at the very high pulling speeds used in SMD.

To illustrate the microscopic nature of the fluctuation that passes the base, the structures of the complex of β-CD and nucleotides are shown at milestones 9, 10, and 11 in Fig. 12. In the transition states, B and E, the bases are flipped over to be parallel to the DNA backbone, passing the CD ring. This explains how a CD can hop quite rapidly ($\sim$100 ns) over the bases with no external force applied. The consequence is that with the measured forces as currently obtained, AFM pulling speeds will be too small to measure, in agreement with the results of a recent experiment (Ashcroft et al., unpublished data).

The predicted forces in Fig. 11 show that even at the high loading rate of 2500 pN/s, the forces are 75–80 pN for passing purines and pyrimidines, and the difference between them is only $\sim$5 pN (less than the AFM noise level). At a normal AFM pulling speed of 100 nm/s with a cantilever stiffness of 0.3 N/m, the forces are essentially zero. To see a significant (above the noise level) force difference between purine and pyrimidine, we need to use a rotaxane molecule, which has a free energy barrier to passage on the order of 20 K_BT. Unmodified bases are not large enough to produce such an increase in the energy barrier, but perhaps modified bases could be a solution to this problem. Another solution could be a smaller pore diameter, i.e., an α-CD, which has six sugar rings and is smaller than a β-CD. Finally, we note that the major limitation on pulling rates with the experimental setup presented here was the fragility of the construct, so more rapid pulling rates might be possible with a different approach to constructing the rotaxane.

The present SMD simulations deal only with transitions across one base because of the time limitations of the method. We have used a geometric technique (33–35) to examine the effects of base stacking on the transition of the CD, and we find significant cooperative motion if bases are stacked (unpublished data).

We thank the sequencing technology program of the National Human Genome Research Institute for support of this work (R21 HG 03061). We also thank Fulton School of Engineering, Department of Geology and Center for Biological Physics at Arizona State University, for providing us the computer resources for this project. We are thankful to Dan Stanzion, Gil Spyer, Austin Godber, and Noel Gorlick for technical support to run this large-scale simulation.

REFERENCES

1. Astier, Y., O. Braha, and H. Bayley. 2006. Toward single molecule DNA sequencing: Direct identification of ribonucleoside and deoxyribonucleoside 5′ monophosphates by using an engineered protein nanopore equipped with a molecular adapter. *J. Am. Chem. Soc.* 128: 1705–1710.
2. Mathe, J., A. Arinstein, Y. Rabin, and A. Meller. 2006. Equilibrium and irreversible unzipping of DNA in a nanopore. *Europhys. Lett.* 73: 128–134.
3. Heng, J., A. Aksimentiev, C. Ho, and P. Marks. 2006. The electromechanics of DNA in a synthetic nanopore. *Biophys. J.* 90: 1098–1106.
4. Heng, J., V. Dimitrov, Y. Grinkova, and C. Ho. 2003. The detection of DNA using a silicon nanopore. Presented in Electron Devices Meeting, IEDM 2003 Technical Digest. IEEE International.
5. Meller, A. 2000. Rapid nanopore discrimination between single polynucleotide molecules. *Proc. Natl. Acad. Sci. USA.* 97:1079–84.
6. Sanger, F., S. Nicklen, and A. Coulson. 1977. DNA sequencing with chain terminating inhibitors. *Proc. Natl. Acad. Sci. USA.* 74:5463–7.
7. Kasianowicz, J. J., E. Brandin, D. Branton, and D. W. Deamer. 1996. Characterization of individual polynucleotide molecules using membrane channel. *Proc. Natl. Acad. Sci. USA.* 93:13770–3.
8. Fologea, D. 2005. Detecting single stranded DNA with a solid state nanopore. *Nano Lett.* 5:1905–1909.
9. Akeson, M., D. Branton, J. J. Kasianowicz, E. Brandin, and D. W. Deamer. 1999. Microsecond time scale discrimination among polycytidylic acid, polyadenylic acid, and polyuridylic acid as homopolymers or as segments within single RNA molecules. *Biophys. J.* 77:3227–33.

10. Spadola, Q., S. Qamar, B. Ashcraft, P. Zhang, and S. M. Lindsay. 2006. Assembly of DNA Rotaxane for AFM Based DNA Sequencing. Cellular Structure and Molecular Dynamic. *Nanotech 2006 Proc*. Boston.

11. Hiroshi, O. 1983. Syntheses and properties of rotaxane complex. *Inorg. Chem.* 23:3312–3316.

12. Bension, R. 2004. Rapid sequencing of polymers. US patent application (2004 0214177).

13. Faradjian, A., and R. Elber. 2004. Computing time scales from reaction coordinates by milestoning. *J. Chem. Phys*. 120:10880–9.

14. Evans, E. 1998. Energy landscapes biomolecular adhesion and receptor anchoring at interface explored with dynamics force microscopy. *Faraday Discuss*. 111:1–16.

15. Qamar, S., B. Ashcraft, Q. Spadola, P. Williams, P. Zhang, and S. M. Lindsay. 2006. DNA Translocation through a Nanopore. Computational Modeling in Life Science. *Nanotech 2006 Proc*. 2:329–332.

16. Cornell, W. 1995. A second generation force field for the simulation of proteins, nucleic acids, and organic molecules. *J. Am. Chem. Soc.* 117:5179–5197.

17. Foloppe, N., and A. MacKerell. 2000. All atoms empirical force field of nucleic acid. *J. Comput. Chem.* 21:86–104.

18. Kalé, L. 1999. Greater scalability for parallel molecular dynamics. *J. Comput. Phys.* 151:283–312.

19. Pearlman, D. 1995. A package of computer programs for applying molecular mechanics, normal mode analysis, molecular dynamics and free energy calculations to simulate the structural and energetic properties of molecules. Comp (AMBER).

20. Jorgensen, W. 1983. Comparison of simple potential functions for simulating liquid water. *J. Chem. Phys*. 79:926–935.

21. Martyna, G. 1994. Constant pressure molecular dynamics algorithms. *J. Chem. Phys.* 101:4177–4189.

22. Berendsen, H. 1984. Molecular dynamics with coupling to an external bath. *J. Chem. Phys*. 81:3684–3690.

23. Feller, S. 1995. Constant pressure molecular dynamics simulation: the Langevin piston method. 103:4613–4621.

24. Allen, M. 1987. Computer Simulations of Liquids. Oxford University Press, New York.

25. Ryckaert, J. 1977. Numerical integration of the Cartesian equations of motion of a system with constraints: molecular dynamics of *n*-alkanes. *J. Comp. Phys.* 23:327–341.

26. Evans, E. 2001. Probing the relation between force-lifetime and chemistry in single molecular bonds. *Annu. Rev. Biophys. Bioeng.* 30:105–128.

27. Kramers, K. 1940. Model of diffusive barrier. *Physica*. 7:284.

28. Smith, S. B., Y. J. Cui, and C. Bustamante. 1996. Overstretching B-DNA the elastic response of individual double-stranded and single-stranded DNA molecules. *Science*. 271:795–9.

29. Karlin, S. 1975. A First Course in Stochastic Simulation, 2nd ed. New York.

30. Montroll, E. 1984. The Wonderful World of Random Walk Nonequilibrium Phenomena.

31. Gillespie, D. 1992. Markov Process. An Introduction for Physical Scientists. Academic Press, San Diego, CA.

32. Evans, E., K. Ritchie, and R. Markel. 1995. Sensitive force technique to probe molecular adhesion and structural linkage at biological interface. *Biophys. J.* 68:2580–2587.

33. Wells, S., S. Menor, B. Hespenheide, and M. F. Thorpe. 2005. Constrained geometric simulation of diffusive motion in proteins. *Phys. Biol.* 2:S127–S136.

34. Sartbaeva, A., S. A. Wells, and M. F. Thorpe. 2006. Geometric simulation of perovskite frameworks with Jahn-Teller distribution. *Phys. Rev. Lett.* 97:065501.

35. Hespenheide, B. M., D. J. Jacobs, and M. F. Thorpe. 2004. Structural rigidity in the capsid assembly of cowpea chlorotic mottle virus. *J. Phys. Condens. Matter*. 16:S5055–S5064.